Coordination Chemistry of a Tripodal S_2ON Ligand: Syntheses, Structures, and Reactivity of the Molybdenum(VI) and Nickel(II) Complexes of Bis(2-mercaptoethyl)-2-amino-4-methylphenol (H_3btap) and Comparison to V^VO(btap)

Charles R. Cornman,*,† Kevin L. Jantzi,† Joseph I. Wirgau,† Thad C. Stauffer,† Jeff W. Kampf,‡ and Paul D. Boyle†

Department of Chemistry, North Carolina State University, Raleigh, North Carolina 27695-8204, and Department of Chemistry, University of Michigan, Ann Arbor, Michigan 48109-1055

Received March 16, 1998

The tripodal tetradentate ligand H_3btap coordinates to V^V, Mo^{VI}, and Ni^{II} *via* three different bonding modes to yield three complexes with unique ligand-based oxidation chemistry. For V^V and Mo^{VI} (**1**), all four of the heteroatom donors are coordinated to the metal ion forming a trigonal bipyramidal complex with the oxovanadium(V) ion, V^VO^{3+}, and an octahedral complex with the *cis*-dioxomolybdenum(VI) ion, $[MoO_2]^{2+}$. Only three of the heteroatom donors of H_3btap are used to coordinate to Ni^{II} (**2**), two thiolate sulfurs and the amine nitrogen, yielding a dimeric structure in which each nickel(II) ion has NS_3 coordination. The ability of V^VO(btap) to form η^2-sulfenates, while $[MoO_2$(btap)$]^-$ does not form stable η^2-sulfenates, has been ascribed to the electron-deficient, π-accepting nature of V^VO^{3+} relative to $[Mo^{VI}O_2]^{2+}$. Crystal data for **1** ($C_{11}H_{16}NO_4S_2KMo$): space group *Pbcn*, $a = 6.6596(9)$ Å, $b = 13.7446(9)$ Å, $c = 32.992(2)$ Å, $\alpha = \beta = \gamma = 90°$, $Z = 8$. Crystal data for **2** ($C_{24}H_{38}N_2O_4S_4Ni$): space group *Pbcn*, $a = 12.0841(3)$ Å, $b = 14.4948(4)$ Å, $c = 16.7751(4)$ Å, $\alpha = \beta = \gamma = 90°$, $Z = 4$.

Introduction

The oxidation chemistry of nickel(II)-thiolate complexes has received much attention over the past decade due to the importance of Ni−SR coordination in nickel hydrogenases[1,2] and carbon monoxide dehydrogenase.[1,3] Darensbourg and co-workers and Maroney and co-workers have demonstrated the formation of nickel-sul*fen*ates (monooxygenate of coordinated sulfur, Ni−S(O)R) and nickel-sul*fin*ate (dioxygenate of coordinated sulfur, Ni−$S(O)_2$R) analogues.[4−11] These ligands are coordinated to the nickel(II) center in an η^1 fashion through the sulfenate (or sulfinate) sulfur atom. Sulfenate and sulfinate formation has been demonstrated for other transition elements;[12,13] however, this chemistry has only recently been demonstrated for early transition metals—this despite the extensive study of molybdenum thiolates in relation to the molybdenum oxotransferases.[14−19] As recently reported, the vanadium(V) complex of bis(2-mercaptoethyl)-2-amino-4-methylphenol, V^VO(btap), which contains two V^V-SR interactions, can be oxidized sequentially to a mono- and disul*fen*ate complex in which the sulfenate ligands coordinate to the metal in an unique η^2 fashion as shown in eq 1.[20,21] To understand the formation of sulfur oxygenates and their coordination modes, we report herein the preparation and characterization of the Ni^{II} and Mo^{VI} complexes of bis(2-mercaptoethyl)-2-amino-4-methylphenol.

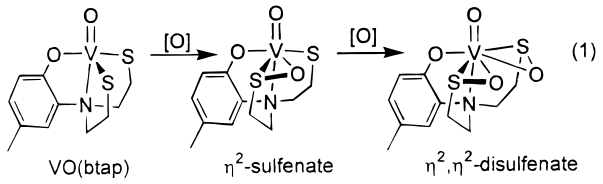

(1)

† North Carolina State University.
‡ University of Michigan.

(1) *The Bioinorganic Chemistry of Nickel*; Lancaster, J. R., Ed.; VCH Publishers: New York, 1988.
(2) Maroney, M. J.; Pressler, M. A.; Mirza, S. A.; Whitehead, J. P.; Gurbiel, R. J.; Hoffman, B. M. *Insights into the Role of Nickel in Hydrogenase*; Thorp, H. H., Pecoraro, V. L., Eds.; American Chemical Society: Washington, DC, 1995; Vol. 246, pp 21−60.
(3) Ragsdale, S. W. *Crit. Rev. Biochem. Mol. Biol.* **1991**, *26*, 261−300.
(4) Maroney, M. J.; Choudhury, S. B.; Sherrod, M. J. *Inorg. Chem.* **1996**, *35*, 1073−1076.
(5) Colpas, G.; Kumar, M.; Day, R. O.; Maroney, M. J. *Inorg. Chem.* **1990**, *29*, 4779−4788.
(6) Mirza, S. A.; Day, R. O.; Maroney, M. J. *Inorg. Chem.* **1996**, *35*, 1992−1995.
(7) Mirza, S. A.; Pressler, M. A.; Kumar, M.; Day, R. O.; Maroney, M. J. *Inorg. Chem.* **1993**, *32*, 977−987.
(8) Kumar, M.; Colpas, G. J.; Day, R. O.; Maroney, M. J. *J. Am. Chem. Soc.* **1989**, *111*, 8323−8325.
(9) Buonomo, R. M.; Font, I.; Darensbourg, M. Y. *J. Am. Chem. Soc.* **1995**, *117*, 963−973.
(10) Darensbourg, M. Y.; Grapperhaus, C. A.; Maguire, M. J. *Inorg. Chem.* **1997**, *36*, 1860.
(11) Grapperhaus, C. A.; Darensbourg, M. Y.; Russell, D. H. *J. Am. Chem. Soc.* **1996**, *118*, 1791−1792.
(12) Nicholson, T.; Zubieta, J. *Inorg. Chem.* **1987**, *26*, 2094−2101.
(13) Sloan, C. P.; Kreuger, J. H. *Inorg. Chem.* **1975**, *14*, 1481.
(14) Dhawan, I. K.; Enemark, J. H. *Inorg. Chem.* **1996**, *35*, 4873−4882.
(15) Enemark, J. H.; Xiao, Z.; Bruck, M. A. *Inorg. Chem.* **1995**, *34*, 5950−5962.
(16) Schultz, B. E.; Gheller, S. F.; Muetterties, M. C.; Scott, M. J.; Holm, R. H. *J. Am. Chem. Soc.* **1993**, *115*, 2714−2722.
(17) Buchanan, I.; Minelli, M.; Ashby, M. T.; King, T. J.; Enemark, J. H.; Garner, C. D. *Inorg. Chem.* **1984**, *23*, 495−500.
(18) Burgmayer, S. J. N.; Stiefel, E. I. *Inorg. Chem.* **1988**, *27*, 2518−2521.
(19) Topich, J.; Bachert, J. O. I. *Inorg. Chem.* **1992**, *31*, 511−515.
(20) Cornman, C. R.; Stauffer, T. C.; Boyle, P. D. *J. Am. Chem. Soc.* **1997**, *119*, 5986−5987.
(21) Cornman, C. R.; Stauffer, T. C.; Boyle, P. D. *Synthesis, Structure, and Reactivity of V^V−Thiolate and V^V−η^2-Sulfenate Complexes*; Crans, D. C., Tracey, A. S., Eds.; American Chemical Society: Washington, DC, 1998; in press.

10.1021/ic9802956 CCC: $15.00
Published on Web 10/07/1998

Experimental Procedures

Materials were purchased from commercial sources and used as received unless otherwise stated. Dry solvents were prepared by distillation from CaH_2 (acetonitrile and hexanes), diphenylketyl radical (THF), or $Mg(OMe)_2$ (methanol) under dinitrogen.[22,23] Acetone was dried via passage through Al_2O_3.

Bis(2-mercaptoethyl)-2-amino-4-methylphenol (H_3btap). Ethylene sulfide (14 mL, 0.12 mol) was added to a refluxing toluene solution (50 mL) of 2-amino-4-methylphenol (5.36 g, 43.5 mmol). The reaction was heated for 40 h at 90 °C. The resulting brownish solution was concentrated to 3 mL *in vacuo*, transferred to a silica gel column, and eluted with a 1:9:27 MeOH/CH_2Cl_2/hexanes solution. The clear, faintly orange fraction was stripped of solvent via rotary evaporation, checked for purity by ^{1}H NMR and used without further purification. ^{1}H NMR (DMSO-d_6) δ (ppm): 2.19 (s, 3 H), 2.49 (under solvent, m, 4 H), 3.16 (m, 4 H), 6.68 (s, 2 H), 6.83 (s, 1 H).

K[Mo^{VI}O$_2$(btap)], 1. $Mo(acac)_2$ (0.32 g, 0.98 mmol) was added to a solution of KOH (0.055 g, 0.98 mmol) and H_3btap (0.24 g, 0.98 mmol) in 100 mL of methanol. This solution was stirred for 40 min and filtered, and the solvent was removed under vacuum. The resulting solid was dissolved in acetone and the residual particulate matter was removed by filtration. Addition of hexanes and evaporation under vacuum yielded **1** as an orange solid in 65% yield. X-ray-quality crystals of **1** were obtained by slow evaporation of an acetone/hexanes solution of **1**. ^{1}H NMR (see Figure S3, acetone-d_6) δ (ppm) for **1**: 2.93 (s, 3H), 3.09 (m, 4H), 3.65 (d of d, 2H), 4.25 (m, 2H), 6.34 (d, 1H), 6.58 (d, 1H), 6.76 (s, 1H). The resonance at $\delta = 2.93$ ppm is assigned to the *p*-methyl protons. The resonances between $\delta = 3.09$ and 4.25 ppm are assigned to the diastereotopic methylene protons of the thioethyl arms and the resonances at $\delta = 6.34$, 6.58, and 6.76 ppm are assigned to the aromatic ring protons.

[Ni^{II}(Hbtap)]$_2$, 2. Under an dinitrogen atmosphere, $Ni(OAc)_2 \cdot 4H_2O$ (215 mg, 0.862 mmol) was added to a 25 mL solution of acetonitrile containing excess H_3btap (236 mg, 0.951 mmol). The light brown solution was stirred for 3 h to produce a fine brown precipitate of **2** in 79% yield. Red/brown X-ray-quality crystals were grown by slow evaporation of a MeOH solution. ^{1}H NMR (see Figure 3; 9:1 CH_2Cl_2/DMSO-d_6) δ (ppm) for **2**: 1.13 (t of d, 2H), 1.68 (d of d, 2H), 2.02 (d of d, 2H), 2.28 (t, 2H), 2.39 (s, 6H), 3.67 (t of d, 2H), 3.87 (d, 2H), 4.39 (d of d, 2H), 5.16 (t of d, 2H), 6.65 (d, 2H), 6.91 (d, 2H), 9.40 (s, 2H), 10.57 (s, 2H). The multiplets between $\delta = 1.13$ and 516 ppm are assigned to the methylene protons of the thioethyl groups. The resonance at $\delta = 2.39$ ppm is assigned to the *para*-methyl protons. The resonances at $\delta = 6.65$, 6.91, and 9.40 ppm are assigned the phenolic ring protons, and the resonance at $\delta = 10.57$ ppm is assigned to phenolic proton.

Physical Measurements. ^{1}H NMR spectra were obtained using a General Electric GN 300 spectrometer using residual solvent protons as an internal reference. UV/vis data were collected on a Hewlett-Packard 8452A diode array spectrophotometer. Infrared spectra were obtained on a Mattson Polaris spectrometer.

X-ray Crystal Structure Analysis. Crystallographic data for **1** and **2** are shown in Table 1. Structural determination for K[Mo^{VI}O$_2$(btap)], **1**, was performed using an Enraf-Nonius CAD4-MACH diffractometer. The sample was maintained at a temperature of 148 K using a nitrogen cold stream. The unit cell dimensions were determined by a fit of 24 well-centered reflections and their Friedel pairs with $28 < 2\theta < 38°$. A unique octant ($+h$, $+k$, $+l$) of data was collected using the omega scan mode in a nonbisecting geometry ($3.0 \le 2\theta \le 50.0°$). Three standard reflections were measured every 4800 s of X-ray exposure time. Scaling the data was accomplished using a five-point smoothed-curve routine fit to the intensity check reflections. The intensity data was corrected for Lorentz and polarization effects. An empirical absorption correction based on psi scans was applied during data reduction. The data were reduced using routines from the NRCVAX set of programs.[24] The structure was solved using SIR92.[25] All non-H atom positions were recovered from the initial *E* map. Subsequent difference Fourier maps yielded peaks suggestive of hydrogen atom positions, however, hydrogen atoms were added at their idealized positions (C−H = 0.96 Å). The phenyl and methylene hydrogens were allowed to ride the parent carbon atom, while the methyl hydrogens and the hydrogens on the water molecule were included as rigid groups. Hydrogen isotropic displacement parameters rode on the parent carbon atom's U_{eq} value according to the expression $U(H) = U(C) + 0.01$ Å^2. All non-H atoms were allowed to refine with anisotropic displacement parameters. The calculated structure factors included corrections for anomalous dispersion from the usual tabulation.[26] The final full-matrix least-squares refinement (based on *F*) converged at $R_F = 0.041$, $R_w = 0.049$ (for data $I_{net} > 1\sigma(I_{net})$). The largest peak in the final difference map was 0.720 e/Å^3. Selected distances and angles for **1** are given in Table 2.

Table 1. Crystallographic Data for K[Mo^{VI}O$_2$(btap)], **1**, and [Ni^{II}(Hbtap)]$_2$, **2**

	1	**2**
empirical formula	$C_{11}H_{16}NO_4S_2KMo$	$C_{24}H_{38}N_2O_4S_4Ni$
fw	425.41	664.22
temperature	148 K	133 K
space group	*Pbcn*	*Pbcn*
a (Å)	6.6596(9)	12.0841(3)
b (Å)	13.7446(9)	14.4948(4)
c (Å)	32.992(2)	16.7751(4)
α, β, γ (deg)	90, 90, 90	90, 90, 90
V (Å^3)	3019.9(5)	2938.27(13)
ρ_{calc} (g cm^{-3})	1.871	1.502
Z	8	4
λ (Mo Kα) (Å)	0.710 73	0.710 73
μ (mm^{-1})	1.40	1.598
R_1[a] (all data)		0.0493
wR_2[b] (all data)		0.0697
R[c] [$I > 1\sigma(I)$]	0.041	
R_w[d] [$I > 1\sigma(I)$]	0.049	

[a] $R_1 = \sum||F_o| - |F_c||/\sum|F_o|$. [b] $(\sum[w(F_o^2 - F_c^2)^2]/\sum[wF_o^4])^{1/2}$. [c] $R = \sum(F_o - F_c)/\sum(F_o)$. [d] $R_w = [\sum(w(F_o - F_c)^2)/\sum(wF_o^2)]^{1/2}$.

Structural determination for **2** was performed using a Siemens SMART CCD-based X-ray diffractometer equipped with a normal focus Mo-target X-ray tube ($\lambda = 0.710\ 73$ Å) operated at 2000 W power (50 kV, 40 mA). X-ray intensities were measured at 133 K and the frames integrated with the Siemens SAINT software package with a narrow frame algorithm. The integration of the data using a primitive orthorhombic unit cell yielded a total of 30307 reflections (between $2.19 \le 2\theta \le 58.82°$) of which 4312 were independent and 3269 were greater than $2\sigma(I)$. The final cell constants (Table 1) were based on the *xyz* centroids of 8192 reflections above $10\sigma(I)$. Analysis of the data showed negligible decay during data collection; the data were corrected for absorption using an empirical method (SADABS) with transmission coefficients ranging from 0.825 to 0.962. The structure of **2** was solved and refined with the Siemens SHELXTL (version 5.03) software package, using the space group *Pbcn* with $Z = 4$ for the formula $C_{24}H_{38}N_2O_4S_4Ni$ which includes one molecule of methanol solvate per asymmetric unit (2 per Ni dimer). All non-hydrogen atoms were refined anisotropically while the hydrogen atoms were allowed to refine isotropically. The final full-matrix least-squares refinement based on F^2 converged at $R_1 = 0.0493$ and w$R_2 = 0.0697$ (for all data); the largest peak in the final difference map was 0.0434 e/Å^3. Selected distances and angles for **2** are given in Table 3.

Results and Discussion

Structures. In the vanadium(V) complex of H_3btap, the ligand adopts a tetradentate, tripodal coordination mode to give

(22) Gordon, A. J.; Ford, R. A. *The Chemist's Companion*; John Wiley & Sons: New York, 1972.
(23) Armarego, W. L. F.; Perrin, D. D. *Purification of Laboratory Chemicals*, 4th ed.; Butterworth-Heinemann: Oxford, 1996.
(24) Gabe, E. J.; Le Page, Y.; Charland, J.-P.; Lee, F. L.; White, P. S. *J. Appl. Crystallogr.* **1989**, *22*, 384−387.
(25) Altomare, A.; Burla, M. C.; Camalli, G.; Cascarano, G.; Giacovazzo, C.; Gualiardi, A.; Polidori, G. *J. Appl. Crystallogr.* **1994**, *27*, 435−436.
(26) *International Tables for X-ray Crystallography*; Ibers, J., Hamilton, W., Ed.; Kynoch Press: Birmingham, England, 1974; Vol. IV.

Table 2. Bond Distances (Å) and Bond Angles (deg) for **1**

Mo−S1	2.4406(16)	S1−C9	1.835(6)
Mo−S2	2.4729(16)	S2−C11	1.834(7)
Mo−O1	1.715(4)	O2−C1	1.343(7)
Mo−O2	2.079(4)	N−C2	1.466(8)
Mo−O3	1.742(4)	N−C8	1.498(8)
Mo−N	2.387(5)	N−C10	1.487(8)
S1−Mo−S2	155.17(6)	C2−N−C10	110.9(5)
S1−Mo−O1	98.38(15)	C8−N−C10	109.7(5)
S1−Mo−O2	83.71(12)	O2−C1−C2	119.7(5)
S1−Mo−O3	94.58(14)	O2−C1−C6	121.8(5)
S1−Mo−N	76.13(13)	N−C2−C1	115.9(5)
S1−Mo−K1	129.46(5)	N−C2−C3	122.9(5)
S1−Mo−K2	92.67(4)	N−C8−H8b	108.8(5)
S2−Mo−O1	103.21(15)	S1−C9−C8	112.3(4)
S2−Mo−O2	82.86(12)	N−C10−C11	110.8(5)
S2−Mo−O3	91.47(14)	S2−C11−C10	111.8(4)
S2−Mo−N	80.14(13)	Mo−S2−C11	100.4(2)
O1−Mo−O2	93.54(19)	Mo−O2−C1	120.4(4)
O1−Mo−O3	105.3(2)	Mo−N−C2	107.6(3)
O1−Mo−N	166.86(19)	Mo−N−C8	105.8(3)
O2−Mo−O3	161.16(18)	Mo−N−C10	109.4(3)
O2−Mo−N	74.13(16)	C2−N−C8	113.2(5)
O3−Mo−N	87.23(18)		

Table 3. Important Bond Distances (Å) and Bond Angles (deg) for **2**[a]

Ni(1)−N(1)	1.997(2)	O(1)−C(6)	1.367(2)
Ni(1)−S(1)	2.1619(6)	O(2)−C(12)	1.409(3)
Ni(1)−S(2)A	2.1824(5)	C(1)−C(2)	1.509(3)
Ni(1)−S(2)	2.2006(5)	C(3)−C(4)	1.508(3)
Ni(1)−Ni(1)A	2.6733(5)	C(5)−C(10)	1.396(3)
S(1)−C(1)	1.828(2)	C(5)−C(6)	1.405(3)
S(2)−C(4)	1.832(2)	C(6)−C(7)	1.394(3)
S(2)−Ni(1)A	2.1823(5)	C(7)−C(8)	1.386(3)
N(1)−C(5)	1.474(2)	C(8)−C(9)	1.389(3)
N(1)−C(2)	1.510(3)	C(9)−C(10)	1.396(3)
N(1)−C(3)	1.516(3)	C(9)−C(11)	1.506(3)
N(1)−Ni(1)-S(1)	92.07(5)	C(5)−N(1)-C(2)	110.5(2)
N(1)−Ni(1)-S(2)A	167.91(5)	C(5)−N(1)-C(3)	110.6(2)
S(1)−Ni(1)-S(2)A	95.98(2)	C(2)−N(1)-C(3)	110.0(2)
N(1)−Ni(1)-S(2)	90.08(5)	C(5)−N(1)-Ni(1)	114.79(12)
S(1)−Ni(1)-S(2)	175.86(2)	C(2)−N(1)-Ni(1)	107.79(12)
S(2)A-Ni(1)−S(2)	81.36(2)	C(3)−N(1)-Ni(1)	102.83(12)
N(1)−Ni(1)-Ni(1)A	115.19(5)	C(2)−C(1)-S(1)	108.4(2)
S(1)−Ni(1)-Ni(1)A	123.75(2)	C(1)−C(2)-N(1)	109.6(2)
S(2)A-Ni(1)−Ni(1)A	52.73(2)	C(4)−C(3)-N(1)	110.3(2)
S(2)−Ni(1)-Ni(1)A	52.106(14)	C(3)−C(4)-S(2)	109.44(14)
C(1)−S(1)-Ni(1)	96.82(8)	C(10)−C(5)-N(1)	118.9(2)
C(4)−S(2)-Ni(1)A	110.47(7)	C(6)−C(5)-N(1)	122.1(2)
C(4)−S(2)-Ni(1)	97.26(7)	O(1)−C(6)-C(7)	121.7(2)
Ni(1)A−S(2)−Ni(1)	75.17(2)	O(1)−C(6)-C(5)	119.3(2)

[a] Symmetry transformations used to generate equivalent atoms: #1, $-x+1, y, -z+{}^3/_2$.

the trigonal bipyramidal complex V^VO(btap).[20] In this geometry, V^VO(btap) can be oxidized to form the six-coordinate η^2-monosulfenate and subsequently the seven-coordinate η^2,η^2-disulfenate (eq 1). In the anionic complex **1**, the $[btap]^{3-}$ ligand coordinates in a tetradentate fashion to the *cis*-dioxomolybdenum(VI), $[(Mo^{VI}O_2)]^{2+}$, unit as shown in Figure 1. The phenolic oxygen, two trans thiolate sulfurs, and an oxo donor define the equatorial plane in this structure. A second oxo donor and the amine nitrogen of the $[btap]^{3-}$ ligand complete the polyhedron. The Mo−heteroatom distances (Table 2) are as expected for a *cis*-dioxomolybdenum(VI) complex.[27]

(27) Average distances are based on a search of the Cambridge Structural Database: Mo−SR, 2.47(9) Å; Mo−O_{oxo}, 1.71(4) Å; Mo−OAr = 2.04(12) Å; Mo−N (tertiary amine) = 2.41(6) Å; Allen, F. H. Kennard, O. *Chem. Des. Autom. News* **1993**, *8*, 31−37.

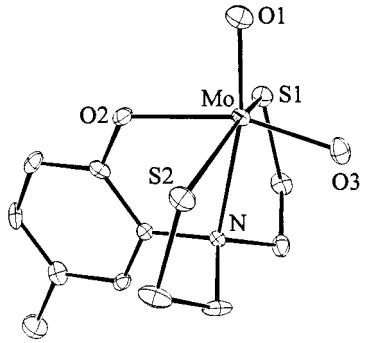

Figure 1. Structural diagram of the anion of **1**, $[Mo^{VI}O_2(btap)]^-$, with thermal elipsoids at the 50% probability level.

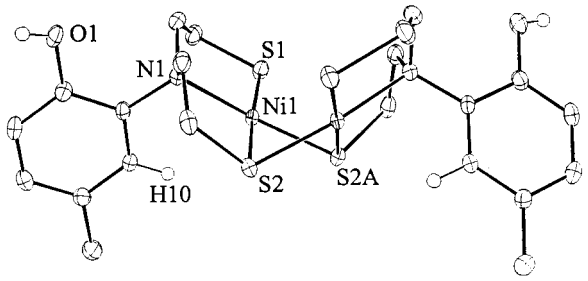

Figure 2. Structural diagram of **2**, $[Ni^{II}(Hbtap)]_2$, with thermal elipsoids at the 50% probability level.

In the neutral nickel dimer **2**, each H_3btap ligand uses only three of the four donor atoms to coordinate to the nearly square planar nickel centers as shown in Figure 2. The largest deviation from the best plane defined by the nickel atom and its four ligands is −0.089 Å observed for the nickel atom. The dimer consists of two such square planar units sharing an edge of their coordination polyhedra. The phenolic oxygen of the ligand is not coordinated and remains protonated as evidenced by ^{1}H NMR spectroscopy (singlet at $\delta = 10.55$ ppm in 9:1 CD_2Cl_2/DMSO-d_6, see Figure 3A) and X-ray crystallography. The nickel atoms in **2** are coordinated by the amine (Ni−N = 1.997(2) Å), a terminal thiolate ($Ni-S_{terminal}$ = 2.1619(6) Å), and two bridging thiolate sulfur atoms ($Ni-S_{bridge}$ = 2.1824(5) and 2.2006(5) Å). The shorter $Ni-S_{bridge}$ distance is to the thiolate sulfur of the second $[Hbtap]^{2-}$ ligand. Similar coordination modes have been observed for other Ni^{II} complexes of *N*-substituted bis(2-mercaptoethyl)amine.[5]

The Ni_2S_2 core of **2** adopts a butterfly geometry. The Ni−Ni distance is 2.6733(5) Å while the S−S distance for the bridging sulfur atoms is 2.86 Å. The fold angle, defined as the angle between the best NiS_2 planes, is 80.5°, which is similar to other Ni_2S_2 core angles. The core S−Ni−S angle is 95.98(2)°, near the ideal 90° expected for a square planar geometry. However, the Ni−S−Ni angle of 75.17(2)° is smaller than expected for sulfur coordination. The alkyl groups of the bridging thiolate ligands adopt a syn-endo geometry, while the phenol substituents on the amine adopt a syn-exo geometry.

Reactivity. The anion of **1**, $[Mo^{VI}O_2(btap)]^-$, is stable under an aerobic atmosphere in many solvents including acetone, acetonitrile, DMSO and water. Complex **1** does react with *m*-chloroperoxybenzoic acid or *tert*-butylhydroperoxide; however, this oxidation results in decomposition of the complex yielding a pale yellow precipitate, and an intractable mixture of ligand-based products. The solid is assigned to the formation of a molybdate oligomer due to its simple infrared spectrum (Supporting Information Figure S4) and the absence of a ^{1}H NMR spectrum in D_2O. Furthermore, upon standing, an NMR sample from the oxidation reaction (in acetone and containing

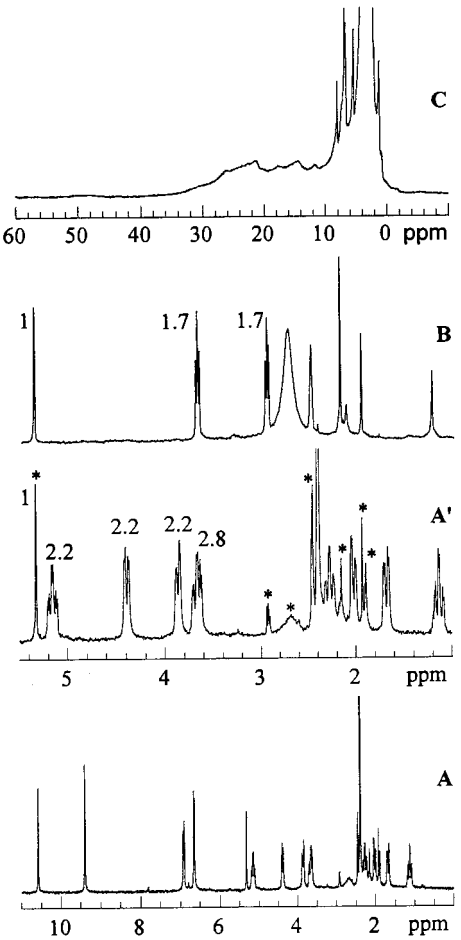

Figure 3. ^{1}H NMR of (A) [Ni^{II}(Hbtap)]$_2$, (A′) expansion of 1−5.5 ppm region of spectrum in A, (B) the air-oxidized solution of [Ni^{II}(Hbtap)]$_2$, and (C) the paramagnetic region of the spectrum in B. Spectra acquired on 9:1 CD_2Cl_2/DMSO-d_6 solutions at ambient temperature using the residual solvent proton from CD_2Cl_2 as an internal standard for chemical shift and intensity. Asterisks if spectrum A′ denote residual solvent protons (5.32 and 2.45 ppm), solvent impurities, and small amounts of the oxidation products (spectrum B).

the yellow precipitate) yielded crystals that were shown by X-ray crystallography to be an acetone solvate of [β-Mo_8O_{26}]$^{4-}$, a known polyoxomolybdate.[28] This structure will be reported separately. The ligand-based products are tentatively assigned to various inter- and intramolecular disulfides.

The neutral nickel dimer, **2**, is stable under dinitrogen and is soluble in THF and DMSO but is only sparingly soluble in most other organic solvents. The ^{1}H NMR of **2** in CD_2Cl_2/DMSO-d_6 (9:1), shown as Figure 3A, is entirely consistent with the solid-state structure. The presence of eight resonances in the 1−5 ppm region of the spectrum (Figure 3A′, assigned to the protons of the thioethyl arms) indicates that the methylene protons are diastereotopic. Therefore, the coordinated tertiary amine is not rapidly inverting on the NMR time scale. The resonance at $\delta = 9.40$ ppm is assigned to H10 (see Figure 2) of the aromatic ring. This downfield shift, relative to the other aromatic protons, suggests that the Ni_2S_2 core has a deshielding effect on H10. Maroney and co-workers have demonstrated that similar nickel dimers react slowly with dioxygen (weeks) to form ligand-oxidized complexes in which the two terminal thiolate ligands, RS^-, are converted to the corresponding sul*fin*ate ligands, $[RSO_2]^-$, as shown in eq 2.[6] Addition of

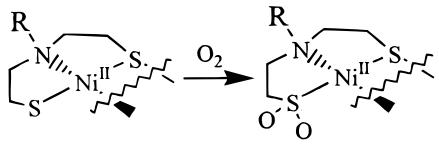
(2)

dioxygen to a solution of **2** (in CD_2Cl_2/DMSO-d_6; 9:1), either as air or pure O_2, results in the rapid conversion (<1 min) of **2** to the disulfide of [Hbtap]$^{2-}$ and a nickel-containing product of unknown composition. The ^{1}H NMR of the resulting solution is shown as Figure 3B. Resonances at 3.0 and 3.7 ppm in Figure 3B are due to the methylene protons of the disulfide (confirmed by independent synthesis). Using the residual solvent protons ($CHDCl_2$) as an internal concentration standard, one finds that free disulfide accounts for only 20−30% of the [Hbtap]$^{2-}$ in the sample (four experiments). (Each of the multiplets in Figure 3A′ corresponds to two protons of the dimer, while the triplet in Figure 3B corresponds to 4 protons of the disulfide derived from [Hbtap]$^{2-}$.) Expanding the NMR sweepwidth (Figure 3C) shows many broad, overlapping resonances between −5 and 50 ppm, strongly suggesting the presence of an $S = 1$ Ni^{II} system. EPR spectroscopy shows a very weak signal at $g = 2$ (singlet) indicating that an uncoupled $S = {}^1/_2$ system is not present in any significant quantity. Attempts to purify the paramagnetic species have been unsuccessful. However, we hypothesize that these paramagnetic complexes contain a disulfide ligand and two additional ligands, perhaps H_2O, as shown in eq 3. The free disulfide observed by ^{1}H NMR (Figure 3B) would then result from dissociation of the disulfide ligand from the complex formed through eq 3.

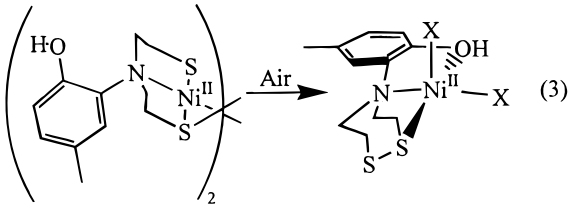
(3)

Formation of a similar complex has been previously demonstrated for the I_2 oxidation of a nickel−thiolate dimer in which the R-group of the complex in eq 2 contains a thioether that coordinates in the final complex.[29] This would suggest that nickel−thiolate dimers of ligands with a surplus donor group are oxidized to disulfide, while those dimers without the surplus donor group are oxidized to sul*fin*ates. The reaction of **2** with I_2 results in the immediate formation of disulfide (analogous to the reaction with dioxygen) and subsequent appearance (over 24 h) of paramagnetically shifted ^{1}H NMR resonances (similar to Figure 3C) between −60 and 50 ppm with multiple sharp resonances in the 10−30 ppm region. The product(s) of the reaction of **2** with iodine are currently under further investigation.

The oxidation chemistry of the ligand is strongly dependent on the electronic structure of the metal complex; late transition metal complexes such as [Ni(Hbtap)]$_2$ react with dioxygen while early transition metal complexes ([MoO_2(btap)]$^-$ and VO(btap)) are stable toward dioxygen but are reactive toward peroxides and peracids. The work of Darensbourg and co-workers[9,10] and

(28) Pope, M. T. *Heteropoly and Isopoly Oxometalates*; Springer-Verlag: Berlin, 1983; p 44.

(29) Kumar, M.; Day, R. O.; Colpas, G. J.; Maroney, M. J. *J. Am. Chem. Soc.* **1989**, *111*, 5974−5976.

Scheme 1

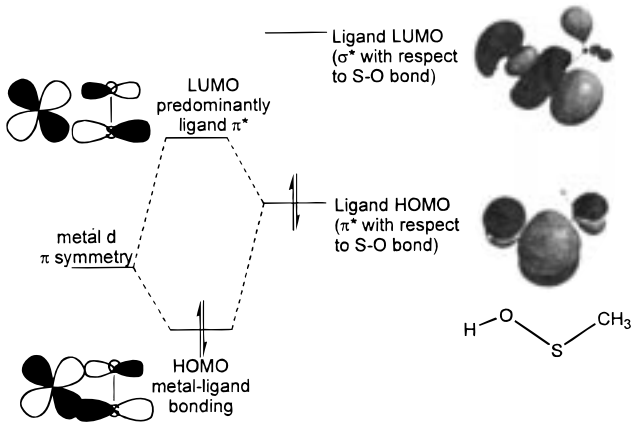

Maroney and co-workers[6,7] has amply demonstrated the dioxygen reactivity of nickel−thiolates, which has been attributed to the nucleophilicity of the sulfur lone pairs of the coordinated thiolate ligand.[4] In the case of early transition elements, which have a d^0 electron configuration, the sulfur lone pairs are involved in π-bonding to the electron deficient metal center, thereby diminishing their nucleophilic character. This being the case, we hypothesize that the oxidant (peroxide or peracid) must be activated, via metal coordination, to react with the coordinated thiol. This hypothesis is currently being explored in this laboratory.

Our inability to convert the octahedral complex $[MoO_2(btap)]^-$ into a stable sulfenate in a manner analogous to VO(btap) is probably due to the higher coordination number in $[MoO_2(btap)]^-$ (6 vs 5 for VO(btap)) and the presence of the second oxo ligand in $[MoO_2(btap)]^-$. The HOMO and LUMO orbitals for methylsulfenic acid (as a peroxide-like tautomer) are presented in Scheme 1.[30] The π^* nature of the HOMO is analogous to that found for peroxide as indicated in most undergraduate inorganic chemistry texts. Side-on η^2-coordination of peroxide ($RO-O^-$) or sulfenate ($RS-O^-$) to an electron deficient metal center such as $[V^VO]^{3+}$ (Scheme 1) removes electron density from these π^* orbitals, thereby stabilizing the ligand. In the case of $[MoO_2(btap)]^-$ the strong π-donation of the second oxo ligand in $[MoO_2(btap)]^-$ may preclude this stabilizing effect leading to reactive sulfenates that proceed to form disulfides. We are currently preparing monooxomolybdenum(VI), $[Mo^{VI}O]^{4+}$, complexes to test this hypothesis.

(30) (a) The electronic structure for MeSOH was calculated using density functional theory (BP86/D**) as implemented in the computational program Spartan. (b) *Spartan SGI*, 5.0.2; Wavefunction, Inc.: Irvine, CA, 1997.

Conclusions

The tripodal tetradentate ligand H_3btap coordinates to V^V, Mo^{VI}, and Ni^{II} *via* three different bonding modes to yield three complexes with unique ligand-based oxidation chemistry. For V^V and Mo^{VI}, all four of the heteroatom donors are coordinated to the metal ion forming a trigonal bipyramidal complex with the oxovanadium(V) ion, $[V^VO]^{3+}$, and an octahedral complex with the *cis*-dioxomolybdenum(VI) ion, $[MoO_2]^{2+}$. Only three of the heteroatom donors of H_3btap are used to coordinate to Ni^{II}, two thiolate sulfurs and the amine nitrogen, yielding a dimeric structure in which each nickel(II) ion has NS_3 coordination. The ability of V^VO(btap) to form η^2-sulfenates, while $[MoO_2(btap)]^-$, **1**, does not form stable η^2-sulfenates, has been ascribed to the electron-deficient, π-accepting nature of $[V^VO]^{3+}$ relative to $[Mo^{VI}O_2]^{2+}$. This is the likely explanation for the absence of the sulfenate structural motif in Mo^{VI}−thiol biomimetic chemistry. With $[Ni(Hbtap)]_2$, **2**, we have observed the oxidative formation of paramagnetic ($S = 1$) Ni^{II} complexes that probably have a disulfide ligand (as opposed to Ni^{II}−sulfenate/sulfinate ligation). We have attributed this reactivity to the availability of the phenolic ligand which can substitute for one of the sulfur donors in the first coordination sphere of the nickel(II) ion. In the biological realm where many potential ligands are present, Ni−sulfenate/sulfinate formation/observation may be precluded due to disulfide formation and subsequent electron-transfer reactions.

Acknowledgment. Funding for this work was provided by the National Science Foundation (CHE-9702873). K.L.J. was supported by an NSF−REU fellowship (CHE-9610196). The X-ray diffractometer at NCSU was purchased using funds from the NSF (CHE-9509532).

Supporting Information Available: Figures S1 and S2 showing full numbering schemes for **1** and **2**, Figure S3 showing the ^1H NMR spectrum of **1**, Figure S4 showing the IR spectra of H_3btap, complex **1**, and the oxidation product of **1**, and tables listing details of crystallographic structures of **1** and **2** (14 pages). X-ray crystallographic files for **1** and **2**, in CIF format, are available on the Internet only. Ordering and access information is given on any current masthead page.

IC9802956